Author Response to Reviews of

Localization control born of intertwined quasiperiodicity and non-Hermiticity

Junmo Jeon, SungBin Lee

RC: ***Report and Comment or Requested changes***, AR: *Author Response*, ☐ Manuscript text

Dear Editor of SciPost Physics,

We thank the referee for giving us comments. Based on the referees' comments, we have completed the response by answering each comment and made changes in the manuscript for clarification. The first referee recommended publication of our manuscript in SciPost Physics. Although the second referee has raised some issues, we believe that all the issues raised by the referee are clarified with additional information and corrections. Thus, we hope our manuscript will be considered as the SciPost Physics.

I. INVITED REPORT 1

RC: I would very much appreciate the response and the corresponding revision of the manuscript. The authors have addressed all of my concerns satisfactorily and revised the manuscript accordingly. I would like to recommend publication of this manuscript in SciPost Physics.

AR: We appreciate the referee for giving a positive comment on our present manuscript.

II. INVITED REPORT 2

RC: I would like to thank the authors for improving their presentation. These improvements have allowed me to better appreciate their work. Given that the issue of relevance is still under discussion, I have read the manuscript once again, and I am afraid that I have identified some further issues.

AR: We appreciate your valuable comments. We have answered to the issues raised by the referee, and improved our manuscript.

RC: In section 3.1, I really had some difficulty following the discussion when rereading it. For example, I was not able to verify statements such as "the delocalization of the state is generally observed" at the top of page 9 or "In particular, Fig.4(c) shows that the extended states disappear in the spectrum due to the non-reciprocal hopping phase" further down on the same page. Indeed, the IPR never goes to zero, i.e., the trends are only qualitative, but there is no strict transition and thus no strict "disappearance". Maybe this is due to the finite system size (finite approximant), and I believe that in order to establish a rigorous conclusion, the dependence on this parameter would have to be investigated. However, I have not even seen this parameter specified in section 3.1.

AR: We thank the referee for detailed review. First of all, "the delocalization of the state is generally observed" is supported by the decrease of MIPR for both $\beta = 0$ and $\beta = 2.5$ with $T = 2\lambda$ (See the red curves in Fig.3 (a) and Fig.4 (a)). The decrease of MIPR indicates that the delocalization of the states in the spectrum has been enhanced.

Next, "Fig.4(c)" should be "Fig.4 (d)" which shows the case of the maximally extended states. Note that if the maximally extended state is the localized state, then there are no extended states. It is because the maximally extended state has minimum value of the IPR. In particular, the sky-colored region in Fig.4 (d) corresponds to the exponentially localized states as we have already specified in the caption of Fig.4. To improve the clarity, we should also emphasize this fact in the main text, and demonstrate the localization of maximally extended state in the sky blue region in Fig.4 (d) in the appendix. The referee suspects that there is no strict disappearance of the extended states, however by investigating the localization properties of the maximally extended state in terms of the minimum value of the IPR in the spectrum, we can numerically specify the conditions where every eigenstate is localized.

The referee also asks the dependence on the system size, N. Although we specified $N = 987$ for Figs.3 and 4, we should emphasize that the characteristics of the change of IPR as the function of N does not change due to the non-reciprocal hopping phase in the AAF model. In other words, the fractal dimensions of the maximally localized and extended states do not change, except the case of the maximally extended states with $T/\lambda < 0.3$ for $\beta = 2.5$. Hence, the change of the system size only changes the whole values of the IPR, that is irrelevant to our main interests. Even for the case of the maximally extended states with $T/\lambda < 0.3$ for $\beta = 2.5$, the localization characteristics change from extended to exponentially localized without exploring the critical state. Since the IPR of the exponentially localized state is independent of N, the changing N only decrease IPR of the extended states. This remains the localization and delocalization behavior as the function of θ shown in Fig.4 (d). Thus, the dependence on the system size, N is irrelvant to our main interests in section 3.1.

Based on the referee's commet, we agree that the further clarifications and explanations are necessary. We modify our manuscript to improve the clarity. For clarification, we emphasize that the sky blue region in Fig. 4 (d) represents the localized state not only in the caption but also in the main text. We also clarify the dependence on the system size N, and its irrelevance to our main interests.

RC: Actually, the biggest difference between the cases $\lambda = 0.2$ and 2 in Figs. 3(a) and 4(a) is the overall scale of the MIPR, but this difference is hidden by using different scales for the two cases. In fact, the biggest difference that I can see between Figs. 3 and 4 is the different shape of the $\lambda = 0.2$ curve in panel (a), but this is in fact a minor effect once the overall scales are considered. I also note that the color scales of panels (c) and (d) might suggest the opposite of what is actually shown (bright colors for small values, lighter ones for large values).

AR: First of all, the different scales between $T = 0.2\lambda$ and 2λ are not significant because depending on the T/λ, the phases are different. For example, as we have explained in the last second paragraph on page 7, for $T/\lambda < 0.5$ and $\beta = 0$, every state is localized for the Hermitian case. On the other hand, for $T/\lambda > 0.5$, every state is extended. These facts for the Hermitian case are already known, thus, the discussion of the scales of the MIPR for different T is not necessary here.

As the referee has pointed out, one of the notable difference between Figs. 3 and 4 is the different shape of the $T = 0.2\lambda$ curve in panel (a). The referee claims that this is a minor effect once the overall scales, however, this is not a minor difference. Although the fraction of the change of MIPR is small, the different types of the change i.e. decreasing and increasing gives totally different results for each state. Specifically, the delocalization of the maximally extended state is observed for $\beta = 0$, while the exponential localization tendency of maximally extended states with varying θ occurs for $\beta = 2.5$ case i.e. localization. Note that the number of extended states, which become localized near $\theta = \pi/2$ for $\beta = 2.5$ is small for the Hermitian case when T/λ is small. Thus, even for the case of $\beta = 2.5$, the fraction of change on MIPR is not large. However, this never means that

the different types of the changes on the MIPR for $\beta = 0$ and $\beta = 2.5$ with $T = 0.2\lambda$ are not important. We emphasize that the different types of the changes on the MIPR capture the totally different localization tendancies of each state as the functions of θ.

RC: In section 3.2, the authors use a different approach from section 3.1 to characterize the $\beta \to \infty$ limit. In fact, reading statements such as "Although a larger IPR indicates stronger localization, the value of the IPR alone is insufficient to determine the detailed localization characteristics and scaling behavior of the wave function, since the IPR is an averaged quantity over space", I could not help wondering why they used exactly the criticized quantity in section 3.1. I think the relation between the approaches needs to be clarified, including the relation between Figs. 3 and 4 on the one side and Fig. 5 on the other side.

AR: We appreciate your comment. Indeed, we think it is better to have more explanation for clarification in the main text. We have not used the fractal dimension in section 3.1 because we do not have any critical states and phase transitions exploring unconventional fractal dimensions. Please note that the fractal dimension is important when there are some fractal wave functions such as the critical states. However, in the AAF model discussed in section 3.1 have either localized or extended states only. Furthermore, although the strength of the localization given by the IPR would be changed, the characteristics of the localization, which are termed by extended, localized and critical are not altered by θ in almost all of the cases. For instance, note that the maximally localized states, which are exponentially localized for $\theta = 0$ remain localized as we have mentioned in the main text. The only case where the fractal dimension changes as θ approaches $\pi/2$ is the maximally extended states for small T/λ regime with $\beta = 2.5$ shown in Fig. 4 (d). However, again even in this case, we have only two trivial kinds of the localization characteristics, localized and extended whose localization characteristics do not have the fractality. Thus, we believe that it is enough to explicitly show the localized and extended states, respectively in the appendix. The landscape of the fractal dimension does not give any further information to the readers in this case. Instead, for clarity, we specify the localization characteristics of the states either exponentially localized ($D_2 = 0$) or extended ($D_2 = 1$) in the captions of Figs 3 and 4.

On the other hand, for the case of the Fibonacci tiling, we have found the important delocalization transition exploring unconventional fractal dimension as shown in Fig. 5. Furthermore, in the case of $\beta \to \infty$, the maximally localized state would be not only localized or extended but also critical states having intermediate fractal dimensions $D_2 \approx 0.5$. Thus, the discussion using the fractal dimension is relevant to the case of Fibonacci tiling only. We agree that it is better to explain the importance of different approaches as the referee commented. We briefly specify the significance of the fractal dimension when we discuss the Fibonacci quasicrystal in the main text.

RC: In section 3.2, the authors also include an analysis of the fractal dimension D_2. They explain that this quantity is derived from the scaling behavior with N, but again they do not specify the values of N that they have used. I also suspect that working with finite N gives rise to numerical errors for D_2. If so, these would have to be specified.

AR: We thank for pointing it out. Based on the referee's comment, we add the information of N values we have used to compute D_2. Surely, the fractal dimension has some numerical errors with finite N. However, such error does not change our results shown in Fig. 5. We also add the detailed numerical results relevant to Fig. 5 in the appendix.

RC: A final, more stylistic remark is that the authors write "we check the grammer and typos carefully, and correct them", I still have some issues with these (actually, this very sentence contains a spelling error). I would prefer to avoid providing a complete list of corrections and thus strongly recommend that they ask a colleague. If they cannot find a native English speaker, e.g., someone from Western Europe should already feel more comfortable with articles.

AR: We thank again for your comment. We have asked one of our colleague who is native in English. Based on his comment, we corrected typos and expressions.

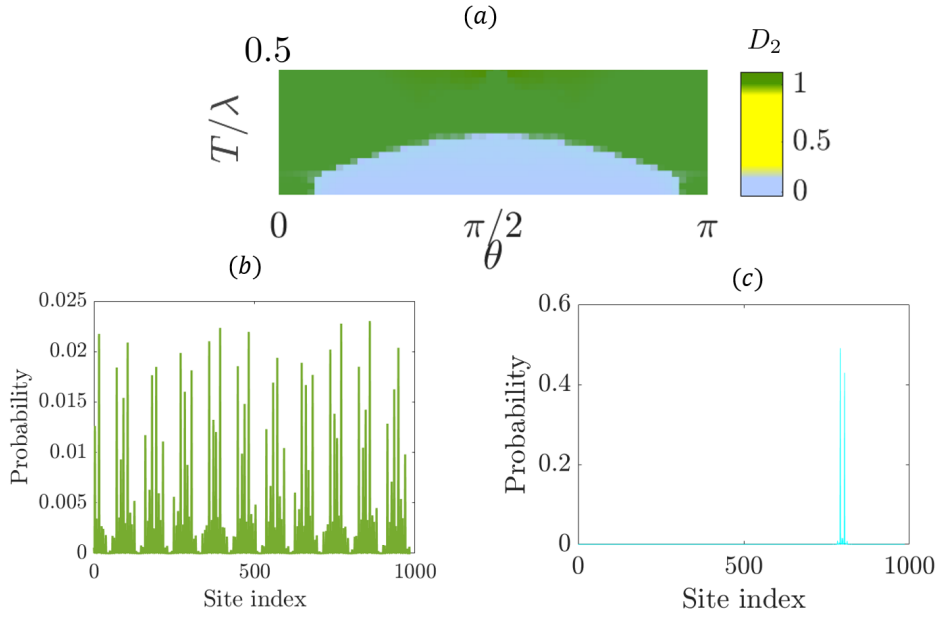

FIG. R.1. Localization of the maximally extended state for $\beta = 2.5$ and $T < 0.5\lambda$. (a) Landscape of the fractal dimension of the maximally extended states. The fractal dimensions are either 0 or 1. The intermediate fractal dimension, colored yellow, does not appear. (b) The extended state for $\theta = 0$ and $T = 0.2\lambda$. (c) The localized state for $\theta = \pi/3$ and $T = 0.2\lambda$. The wave functions are plotted for the system size, $N = 987$. The fractal dimension is calculated using the system sizes from $N = 300$ to $N = 987$.

III. LIST OF IMPORTANT CHANGES

- We specify the size of the system in chapter 3.1, and clarify its insignificance.

  (Added—Caption of Fig. 3 and 4)
  "$N = 987$"

  (Page 7, the last paragraph)
  "$[\cdots]$ of θ. First $[\cdots]$"
  $\rightarrow$ "$[\cdots]$ of θ. We emphasize that although the value of the IPR of an extended state would decrease with increasing system size, the qualitative change of the localization strength as a function of θ is independent of system size. We set $N = 987$. First $[\cdots]$"

- We clarify the transition where the extended states disappear, supported by FIg.4 (d) in the main text.

  (Page 9, the second paragraph)
  "In particular, Fig.4(c) shows that the extended states disappear in the spectrum due to the non-reciprocal hopping phase."
  $\rightarrow$ "In particular, Fig.4 (d) shows that the exponential localization tendency of maximally extended states with varying θ due to the non-reciprocal hopping phase. Specifically, the sky blue region in Fig.4 (d) does not admit the extended states. Note that if the maximally extended state becomes localized, then there is no extended state (see Appendix C for detailed information.)."

  (Add—Appendix B)
  Here, we discuss the localization of the extended states for $\beta = 2.5$ and small T. In particular, we focus on the maximally extended state, which has the minimum value of the IPR in the spectrum. Note that if the maximally extended state becomes a localized state, then every state in the spectrum is localized, i.e. the extended states disappear in the spectrum. Fig.R.1 shows the exponential localization of the extended states for the AAF model with $\beta = 2.5$ and $T < 0.3\lambda$. Fig.R.1(a), which shows the landscape of the fractal dimension

D_2 of the maximally extended state, emphasizes the absence of the extended state in the spectrum as the sky blue region ($D_2 = 0$, exponentially localized). The green region in Fig.R.1(a) indicates the extended states ($D_2 = 1$). Note that the critical states characterized by $0 < D_2 < 1$ (yellow in the color bar of Fig.R.1(a)) do not appear. Fig.R.1(b) and (c) show the typical wave functions corresponding to the green and sky blue regions of Fig.R.1(a), respectively. Thus, as θ approaches $\pi/2$, each eigenstate becomes exponentially localized, and the extended states disappear from the spectrum. Again, we emphasize that there is no critical state during the localization transition due to the non-reciprocal hopping phase.

- We explain the relevant features in Figs. 3 and 4 better, specifying difference and similarities.

  (Page 9, the last paragraph)
  "Comparing Fig.3 and Fig.4, one can conclude that the non-reciprocal hopping phase can either increase or decrease the localization strength depending on the state and the potential distribution depending on β. This implies that the non-reciprocal hopping phase allows for different control of the localization strength. Nevertheless, we find that when the hopping magnitude is sufficiently strong, the delocalization of the states is generally induced. This is because the non-Hermitian interference effect which leads to the effective potential is uniform, and hence for T greater than some critical hopping magnitude, say T_c, the interference in terms of θ uniformly washes out the effects of the potential gradient on the probability distribution, as we demonstrated in the example of an alternating periodic chain."
  $\rightarrow$ "Comparing Fig.3 and Fig.4, one can conclude that the non-reciprocal hopping phase can either increase or decrease the localization strength depending on the state and the potential distribution dependent on β. In particular, Fig.3 (a) and Fig.4 (a) show that when $T = 0.2\lambda$, the change of the MIPR is distinct depending on β. When T/λ is small, for $\beta = 0$, the localization strength decreases, while for $\beta = 2.5$, the localization strength increases as θ approaches $\pi/2$. This implies that the non-reciprocal hopping phase allow different control of the localization strength. Nevertheless, we find that when the hopping magnitude is sufficiently strong, the delocalization of the states is generally induced by decreasing MIPR for both $\beta = 0$ and $\beta = 2.5$ (see the red curves in Figs.3 (a) and 4 (a)). This is because the non-Hermitian interference effect which leads to the effective potential is uniform, and hence for T greater than some critical hopping magnitude, say T_c, the interference in terms of θ uniformly washes out the effects of the potential gradient in the probability distribution, as we have shown in the example of an alternating periodic chain."

- We briefly specify the reason why the discussion using the fractal dimension is relevant to the Fibonacci case ($\beta \rightarrow \infty$). Also, in the captions of Figs.3 and 4, we specify the localization characteristics of the states discussed in section 3.1, either exponentially localized or extended. In detail, every maximally localized states are exponentially localized regardless of β and T/λ. For $T \geq 0.5\lambda$, every maximally extended states are extended. For $\beta = 0$ and $T < 0.5\lambda$, every maximally extended states are exponentially localized. On the other hand, for $\beta = 2.5$ and $T < 0.5\lambda$, the sky blue region indicates the exponentially localized states, while the green and black regions indicate the extended states.

  (Page 11, the last second paragraph)
  "To quantify the localization characteristics of the wave function, we use both the IPR and the fractal dimension of the state. Although a larger IPR indicates stronger localization, the value of the IPR alone is insufficient to determine the detailed localization characteristics and scaling behavior of the wave function, since the IPR is an averaged quantity over space."
  $\rightarrow$ "To quantify the localization characteristics of the wave function in the Fibonacci quasicrystal, we use both the IPR and the fractal dimension of the state. Although a larger IPR indicates stronger localization, the value of the IPR alone is insufficient to determine the detailed localization characteristics and scaling behavior of the wave function, especially the critical state, since the IPR is an averaged quantity over space[1, 2]. Note that for the case of finite β, the localization properties are already well explained by the IPR, since we do not have critical states and phase transitions exploring unconventional fractal dimensions (see Appendix B for detailed information). However, for the Fibonacci quasicrystal given by $\beta \rightarrow \infty$, the critical state would appear with intermediate localization characteristics and unique spatial distribution, such as power-law scaling behavior. Therefore, a more detailed quantification of the different localization characteristics is required. "

- We specify the values of N we used to compute the fractal dimensions. In the appendix, we add the figures to clarify the numerical error (which is minor) of the fractal dimensions. In addition, to satisfy the referee's concern, we also add the error bars on Fig. 7 for the random disordered chain. Note that this error bar is originated from the random disorders. We use 20 samples of random local potential distributions.

  (Add —Caption of Fig. 5)
  "The wave functions are plotted for the system size, $N = 987$. The fractal dimension is calculated using the system sizes from $N = 300$ to $N = 987$."

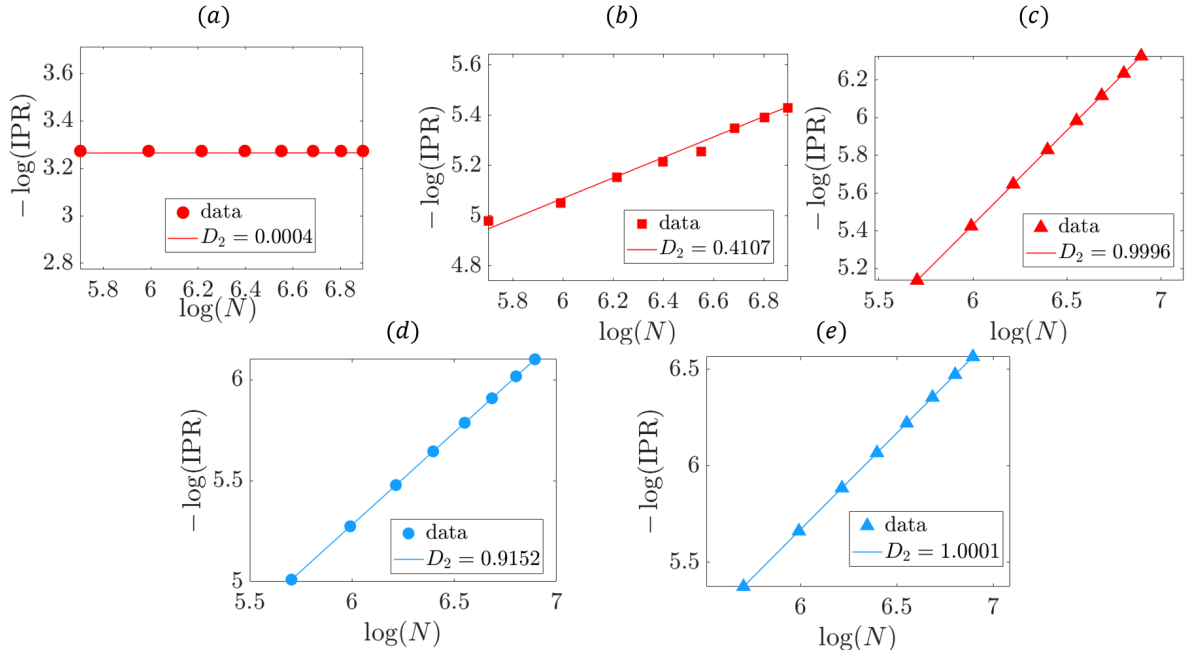

FIG. R.2. Numerical calculation of the fractal dimension with standard error range. The markers correspond to the states illustrated in Fig.5 (b,c,d,g,h). (a) Localized state. $D_2 = 0.0004 \in (-0.0001, 0.0009)$. (b) Critical state. $D_2 = 0.4107 \in (0.4009, 0.4205)$. (c) Extended state. $D_2 = 0.9996 \in (0.9990, 1.0002)$. (d) Critical state. $D_2 = 0.9152 \in (0.9148, 0.9156)$. (e) Extended state. $D_2 = 1.0001 \in (0.9998, 1.0004)$. Here, $N = 300, 400, 500, 600, 700, 800, 900$, and 987. For information on the other parameters, see the main text.

(Add —Appendix D)

Here, we present the detailed numerical calculations of the fractal dimensions. We consider finite system sizes from $N = 300$ to $N = 987$ to extract the power of the scaling behavior of the IPR. For each N value, we calculate the IPR of the maximally localized and extended states, respectively. In Fig.R.2 we show the numerical results of the fractal dimensions of the maximally localized and extended states shown in Fig.5 (b,c,d,g,h). In detail, we compute the fractal dimension of the wave function by applying the linear regression method to $-\log(\text{IPR})$, which is the function of $\log(N)$. The IPR of the localized state would not depend on the system size. On the other hand, the IPR of the critical or extended states would decrease with increasing system size. The fractal dimension can be extracted from the slope of the regression line. The standard error of the fractal dimension is given by the standard error of regression slope. Note that the numerical errors are small enough to distinguish the localized, critical and extended states.

(Replacement —Fig. 7)

- We corrected the typos.

[1] N. C. Murphy, R. Wortis, and W. A. Atkinson, Phys. Rev. B **83**, 184206 (2011).
[2] N. Macé, A. Jagannathan, P. Kalugin, R. Mosseri, and F. Piéchon, Phys. Rev. B **96**, 045138 (2017).

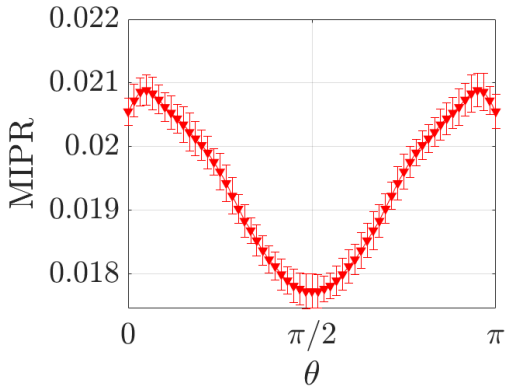

FIG. R.3. MIPR as a function of the phase of the non-Hermitian hopping parameter, θ, in the randomly disordered system. The degree of disorder of the on-site potential energy is 50%. The system size, $N = 233$, and the hopping parameter value, $T = 4V = 4$. The number of samples is 20.